A mathematical foundation of modelling thermal injury and repair dynamics in ectotherms

Andreas Havbro Faber[1,2], Peter Borgen[2], Bodil Ehlers[2], Johannes Overgaard[3], Michael Ørsted[1]

Andreas H Faber[1,2,*] (AHF, faberhavbro@outlook.dk, ORCiD: 0000-0003-3356-7591)
Peter Borgen[2] (PB, pbs@ecos.au.dk, ORCiD: 0000-0003-1338-7198)
Bodil Kirstine Ehlers[2] (BKE, boe@ecos.au.dk, ORCiD: 0000-0002-4712-5025)
Johannes Overgaard[3] (JO, johannes.overgaard@bio.au.dk, ORCiD: 0000-0002-2851-4551)
Michael Ørsted[1] (MØ, moer@bio.aau.dk, ORCiD: 0000-0001-8222-8399)

[1] EcoClimate Modelling group, Department of Chemistry and Bioscience, Aalborg University, Aalborg E, Denmark
[2] Department of Ecoscience, Aarhus University, C.F. Møllers Allé 4, 8000 Aarhus C, Denmark
[3] Section for Zoophysiology, Department of Biology, Aarhus University, Aarhus C, Denmark.
[*] Correspondence: faberhavbro@outlook.dk, Denmark. Phone: +4522198915

Keywords: Ectotherms, Plants, Insects, Heat stress, Injury, Repair, Thermal tolerance, Thermal death time

Abstract

As global temperatures rise and extreme heat events impair ectotherm performance and survival, it is becoming increasingly important to predict how organisms accumulate and repair thermal injury under realistic benign and stressful temperatures. The thermal death time (TDT) model quantifies how heat events translate into thermal injury, but under natural temperature fluctuations the TDT model is inadequate as net injury reflects the balance between injury accumulation during stressful temperatures and repair during permissive temperatures. The relative rates of these antagonistic processes both depend on temperature, and repair also depends on the present level of injury. Empirical evidence of the thermal dependency of both rates remains scarce, and so far, they have not been integrated into mathematical foundational frameworks. Here, we develop two separate modelling approaches to infer these latent processes from thermal failure data for two model organisms: the aquatic plant duckweed (*Lemna gibba*) and the spotted wing fruit fly (*Drosophila suzukii*). First, we introduce a non-parametric TDT model that estimates how temperature exposure contributes to net injury or repair without assuming a predefined temperature response. The model assumes additivity of injury and repair and performs well at identifying permissive and stressful temperatures for the relatively simple *L. gibba* dataset. However, for the more complex *D. suzukii* data, it fails to estimate repair magnitudes because it cannot represent its antagonistic injury dependence. To address this limitation, we introduce a parametric thermal injury-repair model that jointly estimates injury accumulation and repair as antagonistic, temperature dependent latent processes in a probabilistic framework. Here, injury increases exponentially with temperature, while repair follows a unimodal thermal response and depends on accumulated injury through a first order decay process. When applied to the *D. suzukii* data, the model shows that repair can significantly alter rates of injury accumulation under fluctuating temperatures. Together, these approaches provide a framework for translating any temperature history into trajectories of injury and repair. When

55 expanded across different life-stages, more traits and taxa, this will enable predictions of how
56 fluctuating thermal environments shape ectotherm responses to heat extremes and ultimately global
57 warming vulnerability.

Introduction

As climate change increases mean temperatures and the frequency of extreme heat events worldwide, understanding how thermal stress accumulates and affects survival and performance of ectothermic organisms is becoming increasingly urgent (IPCC, 2023). Temperature is a fundamental driver of biological processes in ectotherms, promoting performance at favourable levels while becoming physiologically stressful at extremes impacting survival and lifespan (Angilletta, 2009; Hoffmann & Todgham, 2010; Schulte et al., 2011; Sunday et al., 2011; Diamond, 2017; Malusare et al., 2023; Briceño et al., 2025). Accordingly, at permissive temperatures, organisms can sustain growth, activity, and reproduction (Huey & Kingsolver, 1989; Angilletta, 2009; Fitter & Hay, 2012; Ørsted et al., 2022; Faber et al., 2026a), but when temperatures are stressful, homeostasis of biological processes become disrupted, and their rate of mortality increases (Rezende et al., 2014; Jørgensen et al., 2021; Jørgensen et al., 2022; Ørsted et al., 2022; Cook et al., 2024; Faber et al., 2024). It is becoming increasingly clear that acute heat failure in ectothermic organisms follows an extreme thermal sensitivity when temperatures are stressful (Rezende et al., 2014; Jørgensen et al., 2019; Jørgensen et al., 2021; Ørsted et al., 2022; Cook et al., 2024; Faber et al., 2024; Buckley et al., 2025; Arnold et al., 2025). However, even when extreme temperatures do not result in acute heat failure, accumulated heat stress caused by periodic exposure to stressful temperatures can reduce performance by impairing growth, reproduction, and other biological processes, with lasting effects on fitness (Colinet et al., 2015; Dowd et al., 2015; Kingsolver & Buckley, 2017; Stocker et al., 2024; Vasseur et al., 2014).

When temperatures are consistently stressful, the amount of heat stress an organism accumulates can be expressed as a finite tolerable dose of injury through the thermal death time (TDT) model where log survival time follows a linear relationship with temperature (Rezende et al. 2014; Jørgensen et al.

2019; Jørgensen et al., 2021; Cook et al., 2024; Faber et al., 2024). Assuming injury accumulation is additive in this thermal range, survival time can then be predicted (Fry et al., 1946; Jørgensen et al., 2021; Ørsted et al., 2022; Faber et al., 2024, 2026a; Ørsted et al., 2026). However, predicting how injury accumulates under fluctuating temperatures remains a major challenge, because the amount of injury an organism accumulates emerges from the dynamic balance between the rate of injury accumulation and rate of repair, two antagonistic processes that vary nonlinearly with temperature that can only be estimated indirectly from mortality or other binary thermal failure data, such as heat induced coma (Lutterschmidt & Hutchison, 1997).

These dynamics bear many similarities to modelling frameworks from other disciplines such as the General Unified Threshold model of Survival (GUTS), which have mostly been used to model the toxico-kinetics of chemical stress (Jager et al., 2011; Jager & Ashauer, 2018). In GUTS, the internal concentration of some harmful substance leads to damage – which can be repaired at a certain rate – that in turn leads to mortality. Similarly to thermal stress, as the level of accumulated damage is mostly not measured, we simply observe the endpoints of failure. In this framework, repair is typically represented as a process that is proportional to accumulated injury (Jager & Ashauer, 2018), so that repair can only act on existing injury and higher injury leads to faster repair. Recently, Mangold-Döring et al. (2023) adapted the GUTS framework to thermal stress, explicitly linking injury accumulation and repair as antagonistic processes. In their model, injury accumulates when temperatures exceed a fixed assumed critical threshold temperature, while repair reduces injury at permissive temperatures and is proportional to the current level of injury. However, critically, they assume that the repair rate is independent of temperature. In contrast, Arnold et al. (2025) proposed to combine the TDT model with an estimated temperature-dependent repair function (TPC model) derived from separate recovery experiments (using empirical data from Ørsted et al., 2022). However,

in their framework, injury accumulation and repair are not coupled within a single dynamic state equation as antagonistic processes but instead combined as independently estimated temperature response functions. Using a single fixed recovery duration they also assumed that repair is independent of recovery duration.

Recently, the TDT framework was extended to include a quantitative assessment of repair of thermal injury (Buckley et al., 2025; Ørsted et al., 2026). These studies demonstrate that, at permissive temperatures, repair exceed injury accumulation, allowing organisms to maintain homeostasis, whereas at higher temperatures, injury accumulates faster than repair, ultimately leading to physiological failure. This transition occurs at a critical temperature (T_c), defined as the temperature at which the rates of injury accumulation and repair are equal (Ørsted et al., 2022; Faber et al., 2026a). Repair was shown to be both time-dependent, increasing with longer recovery durations, and temperature-dependent, with low or no repair at cold temperatures, highest near species' optimal temperatures, and a sharp decline at relatively high temperatures, resembling a classic thermal performance curve (TPC) (Buckley et al., 2025; Ørsted et al., 2026). However, in these rather simple experiments, injury and repair rate dynamics were parameterized separately, and did also not consider repair to be mechanistically linked to the current level of injury (i.e., repair is not a function of injury).

There is currently no framework that explicitly couples the temperature-dependent processes of injury generation in a dual model with temperature-dependent, injury-modulated repair inferred from time-resolved mortality data. By explicitly modelling injury generation and repair as antagonistic, temperature-dependent processes, it should be possible to determine the dynamics of these processes in ectothermic organisms directly from any temperature profile and the resulting survival outcomes, even though they cannot be observed directly. Doing so would allow the identification of which temperatures are permissive, which are stressful, where they overlap (T_c) and predicting how rapidly

130 injury accumulates and is repaired through time even when thermal failure is not reached. A key
131 advantage to this is a reduced data demand, as both components can be simultaneously parameterised
132 from relatively simple experimental designs.
133
134 Here we present two different modelling approaches to parameterize these processes. First a non-
135 parametric thermal death time (TDT) model that links injury and repair by estimating their net balance
136 directly from thermal failure data, using the accumulated exposure to different temperatures prior to
137 heat failure. We refer to this model as a non-parametric TDT model because it does not impose an
138 explicit functional form on the temperature dependence of injury and repair but instead assumes that
139 their effects accumulate additively through time with total injury determined by the sum of
140 temperature-specific rates weighted by their exposure durations. By doing so, it reconstructs how
141 thermal history contributes positively or negatively to net injury, thereby mapping permissive
142 temperatures (net repair) and stressful temperatures (net injury). We test this approach on two
143 ectothermic model organisms from different kingdoms, Duckweed (*Lemna gibba*) and the Spotted
144 wing drosophila (*Drosophila suzukii*)
145
146 Building on this approach, and previous work linking the dynamics of injury and repair (Ørsted et
147 al., 2026), we also introduce a parametric model. In this parametric version, injury and repair are
148 represented as two temperature-dependent, antagonistic processes, where injury increases
149 exponentially with temperature and repair follows a unimodal temperature response but, unlike the
150 non-parametric model, also depends on the current level of accumulated injury. By treating both
151 processes as latent and inferring them jointly from thermal failure data, the model captures how their
152 dynamic balance unfolds over time under various temperature histories. Although it requires more
153 data than the non-parametric model, this approach provides mechanistic estimates of injury

accumulation and repair and quantifies their joint uncertainty within a unified probabilistic framework. Due to its higher data requirements, we apply the parametric version only to *Drosophila suzukii*, where sufficiently detailed survival data allow robust estimation of both processes.

The simultaneous injury and repair dynamics can be conceptually thought of as water tank (Fig. 1). In the thermal failure data used by the model, we typically only observe the thermal history and time of failure, while the underlying injury and repair dynamics remain latent (Fig. 1A). These data are then used to infer the processes illustrated in the remaining panels. The inlet of the water tank represents thermal injury, the flow of which represents the rate of injury accumulation (how quickly the tank fills up), modelled as an exponential increase with temperature (Fig. 1B). Conversely, the outlet represents the rate of repair modelled as a peaked Arrhenius function (Fig. 1D). Thus, the water level reflects how net injury accumulates, such that when injury and repair rates are balanced (at T_c), the water level remains constant, whereas net injury accumulates when inflow exceeds outflow. Failure occurs when the water tank reaches its capacity, representing the lethal dose of injury. Similar to Mangold-Döring et al. (2023), we assume that repair follows an exponential decay when the inflow stops (at permissive temperatures). Thus, this concept can also illustrate how repair depends on both temperature and the current level of injury, and how these dynamics affect the decline in injury over time (Fig. 1E-F). Here, at the same amount of injury, repair occurs faster at optimal temperatures, leading to faster decline in net injury (Fig. 1E) and at different amounts of injury sustained, repair is assumed faster the more injury is sustained despite repairing at the same temperature (Fig. 1F). Some unresolved aspects of these dynamics, particularly, the effect of acclimation is also illustrated: long-term acclimation and rapid heat hardening can likely affect both how much injury can be sustained (the volume of the tank), but also directly affect the rates of both injury accumulation and repair (in- and outflow). In other works, these are referred to as increased *tolerance* (tolerable thermal dose) and

178 increased *resistance* (when injury accumulates) (Fry et al., 1946; Cossins & Bowler, 1987; Angilletta,
179 2009; Hoffmann & Todgham, 2010; Ørsted et al., 2022)
180
181 Together, the parametric and non-parametric approaches form a complementary toolkit. The non-
182 parametric TDT model provides a simple but efficient mapping of temperatures that promote repair
183 versus injury, making it useful for descriptive statistical analyses when datasets are relatively simple
184 in structure. In contrast, the parametric model explicitly resolves the underlying physiological
185 dynamics by estimating temperature-dependent injury and repair processes, with repair directly
186 modulated by accumulated injury. This formulation enables reconstruction of injury trajectories and
187 probabilistic prediction of net injury across permissive and stressful temperatures.
188

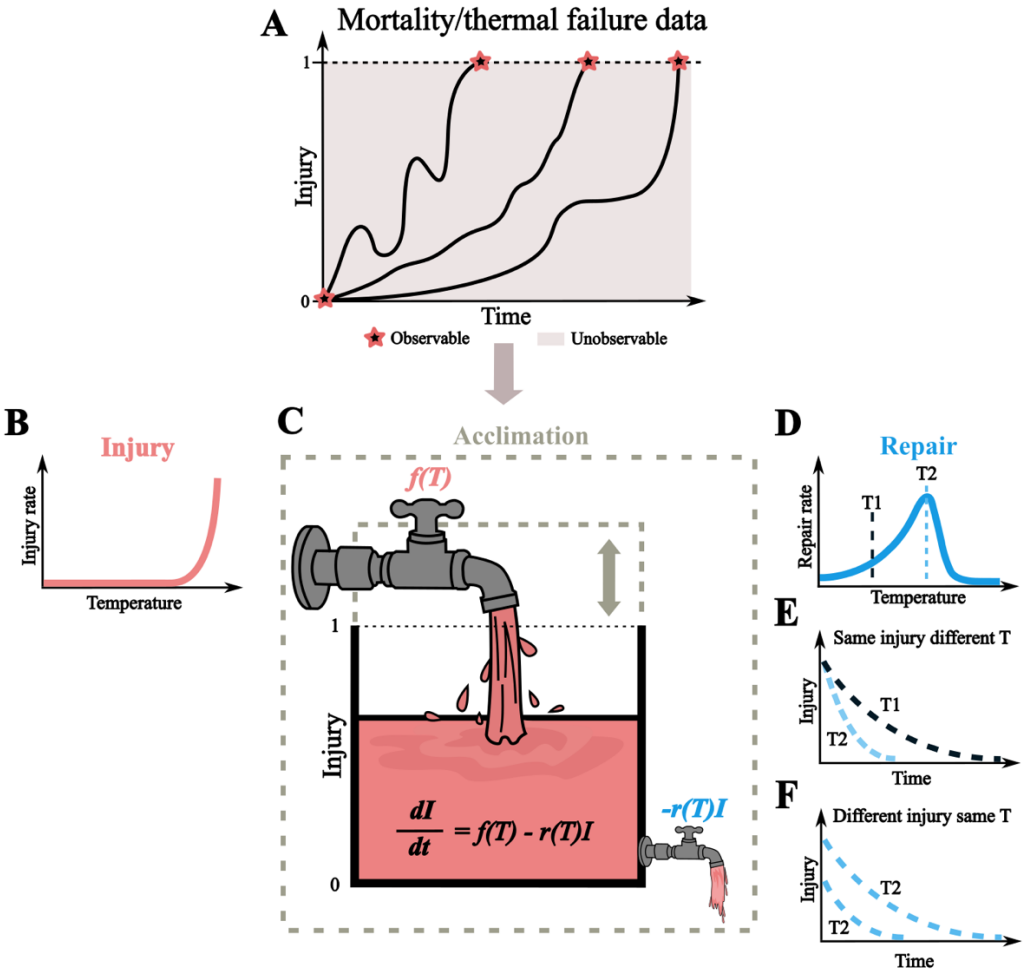

189

190 **Figure 1.**

191 Conceptual framework of the parametric thermal injury–repair model. (A) Observed mortality data consist of the thermal
192 history and time of mortality/thermal failure of an organism. The underlying, injury and repair dynamics are latent. (B–
193 D) the model predicts the temperature dependent rates of injury accumulation (B) and repair (D), where injury increases
194 exponentially with temperature and repair follows a unimodal thermal response. (C) The internal net injury level of an
195 organism is represented as a water tank, where injury influx (inlet) and repair (outlet) determine net injury (water level).
196 When the temperature is stressful and the rate of injury exceeds the rate of repair the water level increases and failure
197 occur when a critical injury threshold (tank capacity) is reached. Acclimation or hardening responses may potentially
198 modify this system by affecting injury rates, repair rates, or the lethal threshold (i.e. inlet, outlet, or tank volume). (E–F)
199 Repair reduces accumulated injury as an exponential decay over time and depends on temperature (E) and current injury
200 load (F), reflecting the antagonistic coupling between injury and repair processes in the model. Together, these
201 components determine net injury dynamics under fluctuating temperatures.

Methodology

Photosynthetic thermal failure data for *Lemna gibba*

We used data for *Lemna gibba* from Faber et al. (2026a), comprising three different experiments: constant, ramping, and alternating temperature assays (Fig. 2). In this system, thermal failure was quantified at the population level based on photosynthetic thermal failure. Accordingly, thermal failure was estimated as the time to induce a 50% reduction in the maximum quantum efficiency of photosystem II (F_v/F_m) on the population level, providing an Et_{50} measure derived from chlorophyll fluorescence to represent thermal failure (Faber et al., 2026a).

The dataset for this species comprises constant temperature assays within the stressful temperature range (Fig. 2A), linear ramping assays where the ramp speed is fixed but vary based on the starting temperatures of the ramps (Fig. 2B), and alternating assays consisting of an initial high stressful temperature exposure followed by a period at lower "repair" temperatures before re-exposure to the initial stressful temperature (Fig. 2C). These assays comprise a range of thermal histories, from constant to dynamically fluctuating temperature profiles, enabling inference about which temperatures contribute to net injury or repair over time (Faber et al., 2026a). The dataset containing all temperature profiles for all assays can be found in **supplementary data S1** and details on population maintenance can be found in Faber et al., 2026a.

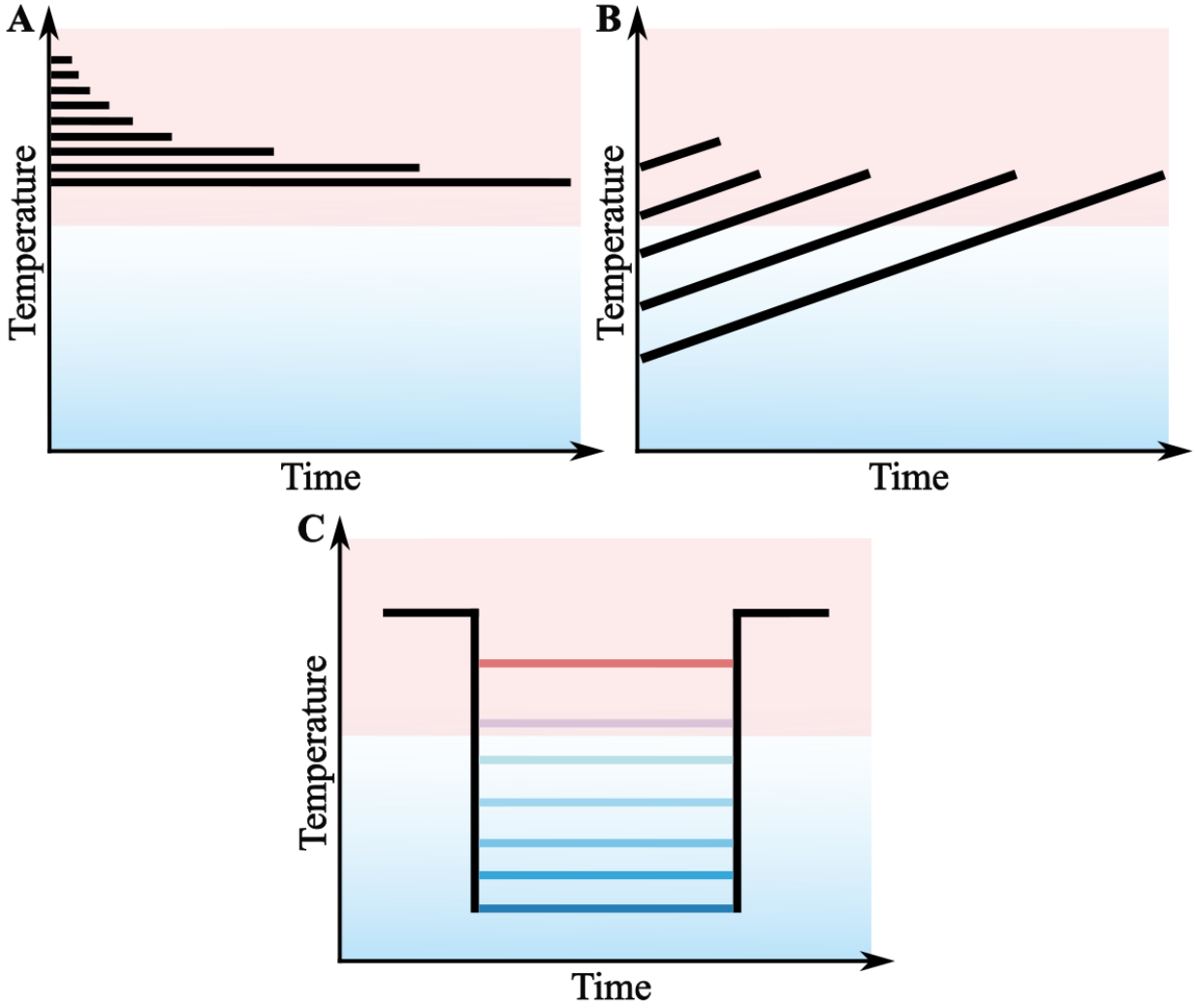

Figure 2.

Conceptual figure of the thermal tolerance assays used to estimate net thermal injury accumulation in *L. gibba* (data from Faber et al., 2026a). The assays include constant temperature assays (**A**), ramping temperature assays where the temperature increases in a linear fashion from different starting temperatures (**B**), and alternating temperature treatments with transitions between stressful and permissive temperatures (**C**). Thermal failure was estimated for all assays the time when a 50% reduction in the maximum quantum efficiency of photosystem II (F_v/F_m) occurred on a population level, indicating significant photosynthetic injury. The red and blue shaded areas in the panels indicate stressful and permissive temperatures, respectively.

Heat knockdown data for *Drosophila suzukii*

We used data on heat knockdown time as a measure of thermal failure for male *Drosophila suzukii* from Ørsted et al. (2026), consisting of a set of constant and fluctuating temperature experiments (Fig. 3). In contrast to the *L. gibba* experiments, thermal failure in *D. suzukii* was measured at the individual level as the time at which flies entered coma, defined as the loss of movement in response to stimulation. Although heat coma precedes mortality, i.e., recovery may be possible after coma if the stress is quickly relaxed, it provides a robust and widely used proxy for acute thermal failure in insects and allows estimation of individual failure times.

The dataset for this species comprised a range of five experimental designs that varied both in the intensity and temporal structure of thermal exposure which allows parametrisation of the temperature response of injury and recovery as well as their interaction. Experiment 1 included constant temperature assays where flies were exposed to eight stressful temperatures (Fig. 3A). Experiment 2 were two-step assays where flies were transferred between constant stressful temperatures, either decreasing or increasing between two levels (Fig. 3B) with varying exposure duration at each temperature step. Experiment 3 included more complex alternating thermal regimes combining three stressful temperatures with six to seven lower "recovery" temperatures, with variation in the exposure duration of both phases (Fig. 3C).

Experiment 4 allowed flies to undergo recovery in more dynamic conditions where flies were exposed to a stressful temperature followed by a drop to permissive temperatures, after which the temperature was either decreased further or increased to another permissive temperature before being returning to the initial stressful temperature (Fig. 3D). Lastly in experiment 5, flies experienced repeated cycles of stressful temperature interspersed with 6-hour recovery periods at three different repair

253 temperatures (Fig. 3E). The dataset containing each temperature profile for all flies in each
254 experiment across all assays can be found in **Supplementary data S2**. Here 5-10 flies were used pr.
255 repetition of each experiment adding up to 998 flies used across all experiments. Further details on
256 the origin and maintenance of the population can be found in Ørsted et al, (2026).
257

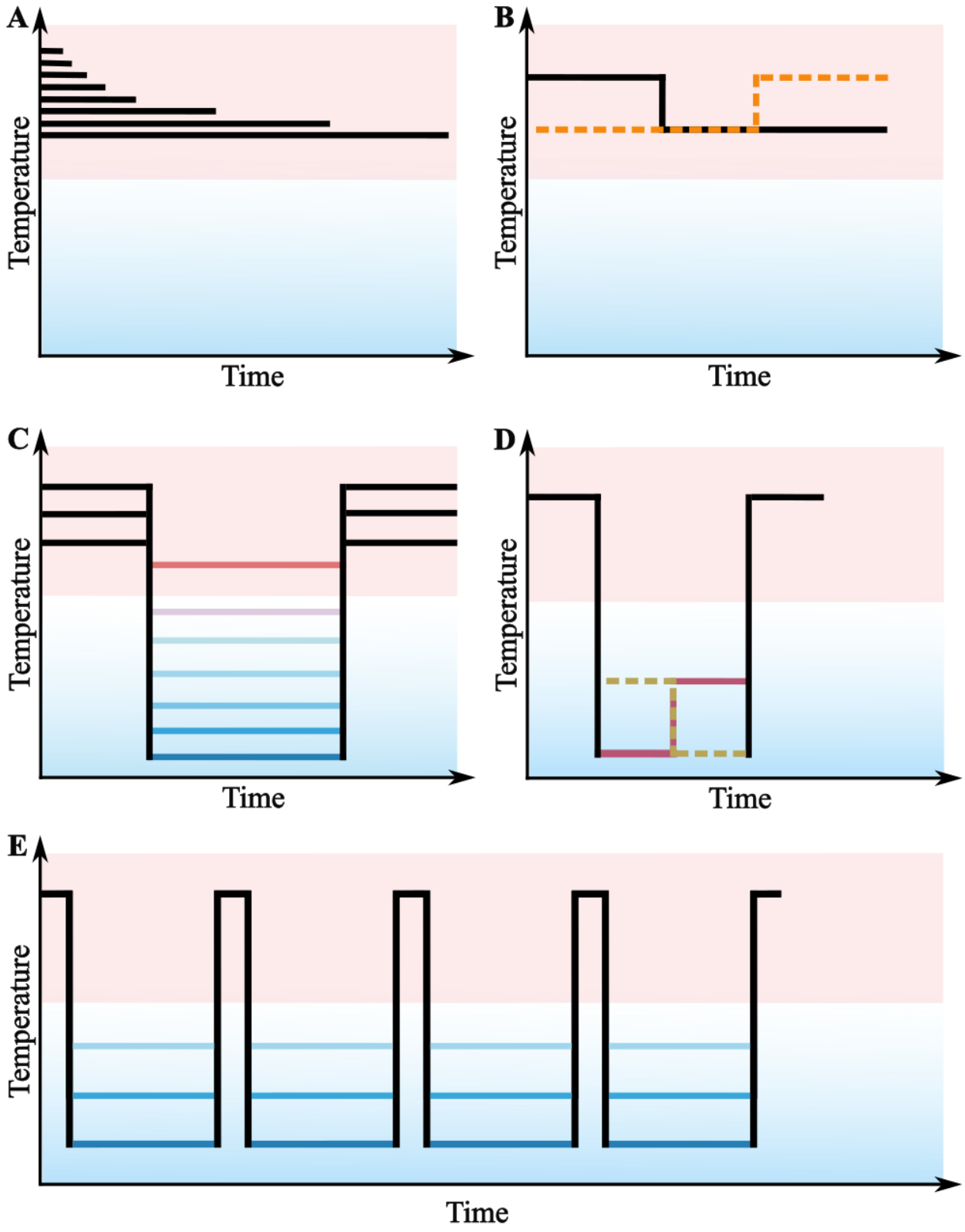
A
Temperature
Time
B
Temperature
Time
C
Temperature
Time
D
Temperature
Time
E
Temperature
Time

258

Figure. 3.

Conceptual figure of the thermal tolerance assays used to estimate net thermal injury accumulation in *D. suzukii* (data from Ørsted et al., 2026). (**A**) Constant temperature assays at eight stressful temperatures. (**B**) Two-step temperature assays with shifts between constant stressful temperatures (decreasing or increasing). (**C**) Alternating temperature assays combining three stressful temperatures with six to seven recovery temperatures. The exposure duration at the high and low temperatures varied within and across each experiment. (**D**) Stepwise recovery assays in which the temperature is reduced from a stressful to a permissive temperature before returning to initial stress temperature, with two alternative recovery temperature trajectories. (**E**) Cyclic assays with repeated exposures to a stressful temperature interrupted with 6-hour recovery periods at a permissive temperature. Thermal failure was measured at the individual level as the time or temperature at which flies entered heat coma. The red and blue shaded areas in the panels indicate stressful and permissive temperatures, respectively.

The non-parametric TDT model

The non-parametric TDT model assumes that thermal injury and repair accumulate additively over time, with temperature-specific rates. In this model, each discrete temperature T_i an organism experience is associated with a parameter β_i, representing the net rate of injury accumulation per unit time at temperature T_i. These parameters may be positive (reflecting injury) or negative (reflecting repair). Each replicate corresponds to an exposure history for either an individual (*D. suzukii*) or a population mean (*L. gibba*) where time of failure is recorded. For each replicate, cumulative injury is calculated as the sum of contributions across all temperatures, weighted by the duration of exposure at each temperature.

The model is fitted across all replicates with different exposure histories, allowing the shared parameters β_i to be estimated jointly. Thermal failure is assumed to occur when cumulative injury

reaches a fixed threshold, which is normalised to 1 across replicates. No intercept is included, so all replicates begin at zero injury. The model is defined as:

$$I_j = \sum_{i=1}^{k} \beta_i t_{ij} + \varepsilon_j \quad \text{(Eqn. 1)}$$

Where t_{ij} is the time spent at temperature T_i in replicate j, k is the number of discrete temperature bins, and $\varepsilon_j \sim N(1, \sigma^2)$ is the residual variation. Under the assumption that I_j= 1, this expression be formulated as:

$$1 = \sum_{i=1}^{k} \beta_i t_{ij} + \varepsilon_j \quad \text{(Eqn. 2)}$$

This expression allows each β_i to be estimated independently, with the number of parameters increasing with the number of temperature bins. Hence, there is no assumption about how injury or repair rates vary with temperature. In this study we fit the model separately to the full dataset of *L. gibba* and *D. suzukii*. To maintain model identifiability, the number of temperatures across all experiments within each species are grouped into bins so that, temperatures are rounded to a predefined set (for *L. gibba* temperatures were binned to 26, 30, 34, 35, 36, 37, 38, 39, 40, 41, 42, 43, 44, and 45 °C and for *D. suzukii* temperatures were binned to 10, 14, 18, 22, 26, 30, 34, 34.5, 35, 36, 36.5, 37, 37.5, and 38 °C), with finer resolution at higher temperatures where injury rates change rapidly at even small temperature changes, and with less resolution at lower temperatures where rates are much less temperature sensitive (Ørsted et al., 2022; Ørsted et al., 2026). This assumes that temperatures rounded to the nearest bin have the same injury or repair rates. In practice, the model requires at least one more replicate than the number of temperatures bins to ensure identifiability of the model. An R-script where the model is fitted to the *L. gibba* dataset is shown in the **supplementary R-code (R1)**.

The parametric thermal injury repair model

The parametric model predicts net injury as a dynamic balance between temperature dependent rates of injury and repair. Since this model requires a dataset that reflects both the temperature dependence of both processes and how repair depends on different levels of injury, we only fit it to the *D. suzukii* dataset. Net accumulated injury at a given time can be described as $I(t)$, and the temporal dynamics of injury accumulation can be denoted as a first-order differential equation:

$$\frac{dI}{dt} = f(T) - r(T)I \quad \text{(Eqn. 3)}$$

Where $f(T)$ is the temperature dependent injury rate and $r(T)$ is the temperature dependent repair rate, which is multiplied by the amount of accumulated injury *I,* meaning that repair acts in a state-dependent manner proportional to the current injury load, such that recovery is consistent with first-order kinetics. Injury is assumed to increase exponentially with temperature accordingly:

$$f(T) = \exp\left(\beta(T - \alpha)\right) \quad \text{(Eqn. 4)}$$

Where β representes thermal sensitivity and α represents an intercept-scaling parameter. Repair is defined using a peaked Arrhenius function, which captures an increase in repair rate with temperature up to an optimum, followed by a decline at higher temperatures due to thermal inactivation:

$$r(T) = r_{ref} \cdot \frac{\exp\left(-\frac{E}{k}\left(\frac{1}{T_k} - \frac{1}{T_{ref}}\right)\right)}{1+\exp\left(\frac{E_h}{k}\left(\frac{1}{T_h} - \frac{1}{T_k}\right)\right)} \text{(Eqn. 5)}$$

Where T_k= T+ 273.15 is the temperature in Kelvin, k = 8.617×10^{-5} eV K^{-1} is the Boltzmann's constant and T_{ref} = 293.15 K (20 °C) is the reference temperature. The parameter r_{ref} is a scaling parameter governing repair rate at the reference temperature, E is the activation energy of repair, E_h is the high-temperature deactivation of repair and the parameter T_h defines the temperature at which high-temperature deactivation becomes critical. The temperature dependent net injury accumulation is then determined over each temperature interval the organism experiences until thermal failure. For

each interval of duration Δt at a given temperature T, the analytical solution to the differential (eqn. 3) can be expressed accordingly:

$$I(t+\Delta t) = \frac{f(T)}{r(T)} + \left(I(t) - \frac{f(T)}{r(T)}\right) e^{-r(T)\Delta t} \quad \text{(Eqn. 6)}$$

Where thermal failure occurs when the accumulated injury is equal to 1. From mortality data the final observed injury (I =1) is then modelled as:

$$I_{obs} = 1 + \varepsilon, \qquad \varepsilon \sim N(0, \sigma^2) \quad \text{(Eqn. 7)}$$

The model parameters are estimated with maximum likelihood across all exposure profiles. The model was implemented in R using the RTMB package, which provides an R interface to Template Model Builder (TMB; Kristensen et al., 2016). The user defines the joint negative log-likelihood function and the random effects as a function in R and the package evaluates and maximizes the Laplace approximation of the marginal likelihood where the random effects are automatically integrated out. This approximation, and its derivatives, are obtained using automatic differentiation (up to order three) of the joint negative log-likelihood. The computations are designed to be fast for problems with many random effects and parameters. To improve identifiability and prevent biologically unrealistic solutions, parameters were constrained to biologically plausible ranges during optimisation (Table S1).

To test whether accounting for repair at permissive temperatures is statistically significant we compared the full model to a reduced injury-only model where injury accumulates as *dI/dt = f(T)* without the inclusion of a repair term. The two models were compared using a likelihood ratio test and statistical significance was evaluated against a chi-squared distribution with degrees of freedom equal to the number of parameters in the full model ($\beta, \alpha, r_{ref}, E, E_h,$ and T_h).

Predictions with the estimated model parameters of the full model was conducted using Monte Carlo simulations by sampling random draws from a multivariate normal distribution defined by the maximum likelihood estimates of the parameters and their covariance matrix. For each parameter draw, injury trajectories were simulated by iteratively applying the analytical solution of the model (eqn. 6) across temperature profiles. This yielded a distribution of injury trajectories, from which the median predictions and 95% CI were obtained at each time point. This approach accounts for the joint parameter uncertainty of the model and how this uncertainty accumulates through time. An R-script where the model is fitted to the *D. suzukii* dataset and examples of how to make predictions with the model is shown in the **supplementary R-code (R2)**.

Results

The non-parametric TDT model

The non-parametric TDT model estimated temperature specific injury and repair rates, revealing stressful and permissive temperatures across all experiments for both species (Fig. 4). Overall, the model enabled a consistent identification of stressful and permissive temperatures within a unified analytical framework across very diverse datasets (Fig. 2 and 3).

For *L. gibba*, all β_i estimates, representing the net rate of injury accumulation at each temperature, were non-negative and thus no temperatures across the experiments were associated with significant repair for this species (Fig. 4A). Injury rates were not significantly different from zero at temperatures below 36 °C. All temperatures at and above 36 °C resulted in significant injury rates that increased exponentially with temperature.

For *D. suzukii*, the β_i estimates varied across the temperature range of the experiments, with both injury and repair detected (Fig. 4B). Significant positive injury rates were observed between 34 °C and 38 °C, increasing exponentially with temperature. In addition, 10 °C and 14 °C resulted in significant injury according to the model. Temperatures outside these ranges did not result in significant injury, while 22 °C and 26 °C resulted in significant negative β_i estimates, reflecting repair.

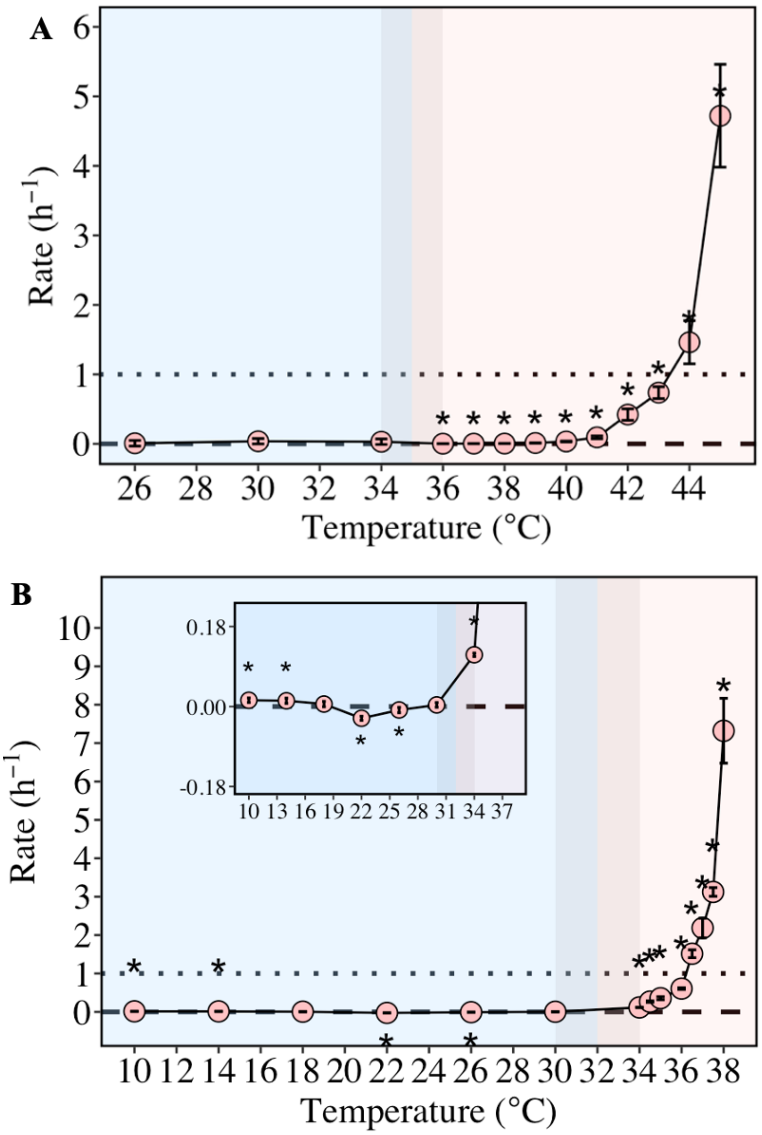

Figure 4.

Estimated injury and repair rates (β_i, hour^{-1}) of the non-parametric thermal death time (TDT) model for (A) *L. gibba* and (B) *D. suzukii*. Points represent estimated β_i parameter values for each temperature bin for each species, with error bares indicating the parameter uncertainty ± 95% CI. Asterisks indicate parameter estimates of injury or repair rates that are significantly different from zero ($P < 0.05$) and the red and blue shaded areas indicate estimated stressful and permissive temperatures, respectively, while their overlap represents the transition zone from no injury to injury. The dotted horizontal line in both panels indicate the rate of injury that result in thermal failure after one hour exposure time.

The parametric injury-repair model

The latent injury and repair trajectories for *D. suzukii* were estimated (eqn. 6) such that the time of thermal failure was predicted with an RMSE value of ± 0.24 across the full dataset. Importantly, the model including temperature and injury dependent repair (eqn. 5) provided a significantly better fit than the reduced model with only injury included (eqn. 4; likelihood ratio = 427.03, $P < 0.05$). Parameter estimates for the full model are given in Table S1. The model estimated instantaneous rates of injury and repair and their antagonistic interaction across temperatures (Fig. 5A). The rate of injury increased exponentially with temperature and was equal to the instantaneous rate of repair at a median of 32.02 °C (95% CI = 31.62 – 32.61 °C), representing T_c. In contrast repair followed a unimodal response, with highest rates at intermediate temperatures (~24 °C), and declining at higher temperatures. Relative repair rates from the alternating stressful and permissive temperatures experiment (Fig. 3C) are shown in Fig. 6 which support the model's assumption that injury exhibits an exponential decay as recovery occurs at different permissive temperatures through time. However, this relationship clearly depends on the recovery temperature.

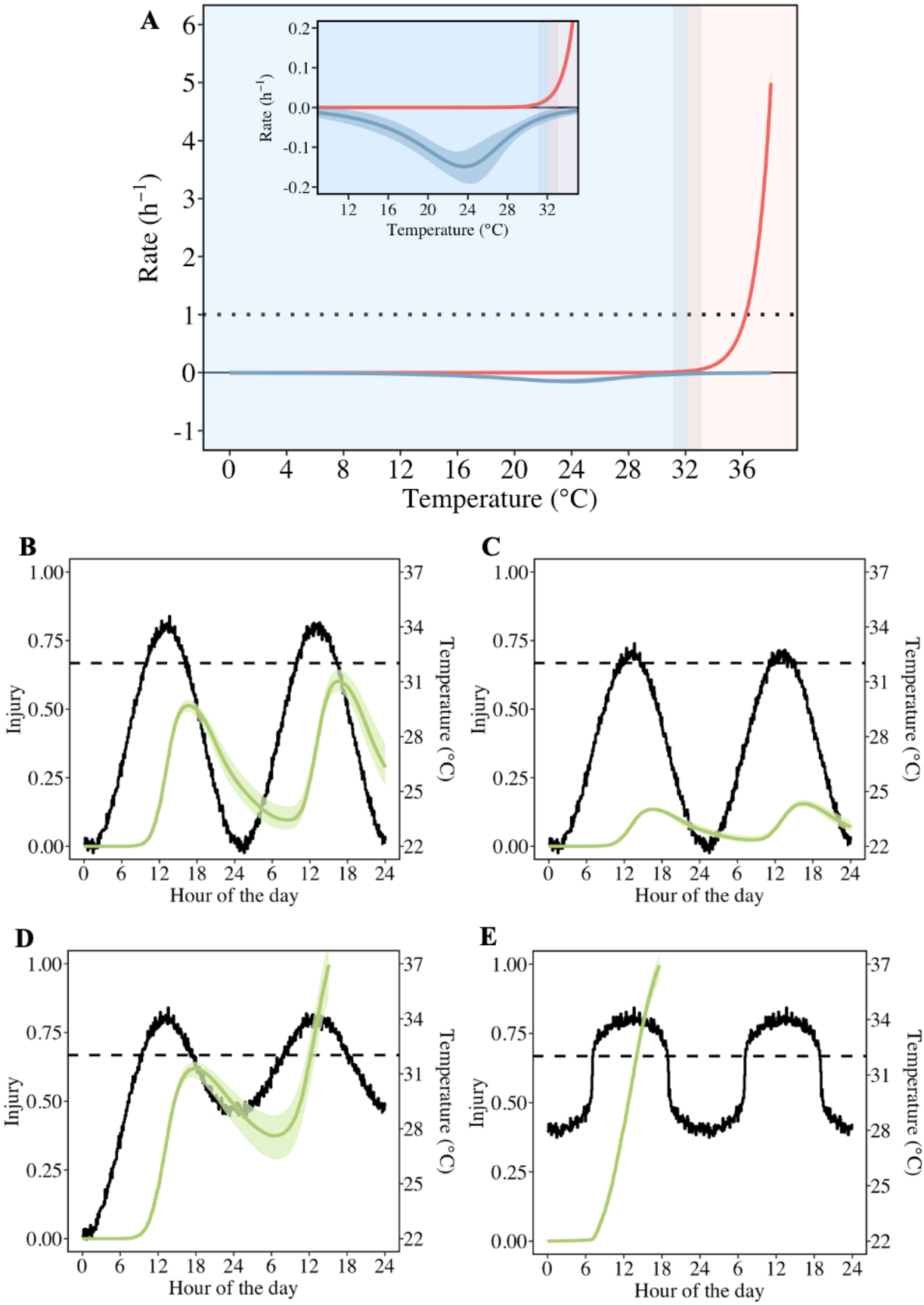
A
Rate (h^{-1})
Temperature (°C)
B
C
D
E
Injury
Temperature (°C)
Hour of the day

402

Figure 5.

The temperature dependent injury and repair rates (hour^{-1}) predicted by the parametric thermal injury repair model for *D. suzukii*. (A) the instantaneous rates of injury (red) and repair (blue) as functions of temperature. Solid lines represent the estimated rates based on maximum likelihood estimation of the model parameters, and bands around the solid lines indicate pointwise 95% CI bands. Injury rates increase as a function of temperature in an exponential fashion, whereas repair follows a unimodal response, where repair reaches its maximum at 24.50 °C and declines at higher temperatures. The dotted horizontal line indicates the rate of injury that result in thermal failure after one hour exposure time. The intersection between injury and repair rates defines the critical temperature (T_c ~ 32.13 °C), above which net injury accumulation occurs. (B-E) illustrates the predicted injury dynamics under fluctuating temperature regimes for *D. suzukii*. The left y-axis depicts net injury, the x-axis reflects hour of the day, the black lines show the temperature profiles (right y-axis) and the dotted horizontal lines illustrate T_c. The green lines illustrate the median predicted accumulated injury over time, and shaded areas indicate 95% CI bands estimated with Monte Carlo simulations. Predictions were generated by iteratively solving the analytical model (eqn. 6) across the temperature profiles where the shaded CI bands reflect the propagated parameter uncertainty in injury trajectories. The simulations were capped when the median accumulated injury reached the thermal failure threshold (injury = 1). The different panels illustrate how variation in daytime and night-time temperatures affects net injury through the balance between injury and repair, leading to full recovery (B-C) carryover effects (D), or rapid thermal failure (E).

Predictions with the parametric model under simulated daily fluctuating temperatures demonstrated how injury and repair determine net injury over time based on the estimated parameters (Fig. 5B-E). Across days, when temperatures exceed T_c but drop sufficiently during the night, accumulated injury is partially repaired between daytime heat exposures (B) but under even lower daytime heat exposure amplitudes injury is much lower (C). In contrast, for elevated night-time temperatures (D) reduced repair leads to incomplete recovery and results in carryover effects of injury accumulation across days, ultimately resulting in thermal failure. When daytime temperatures are higher for longer durations (E), injury accumulates rapidly and thermal failure occurs within a single day.

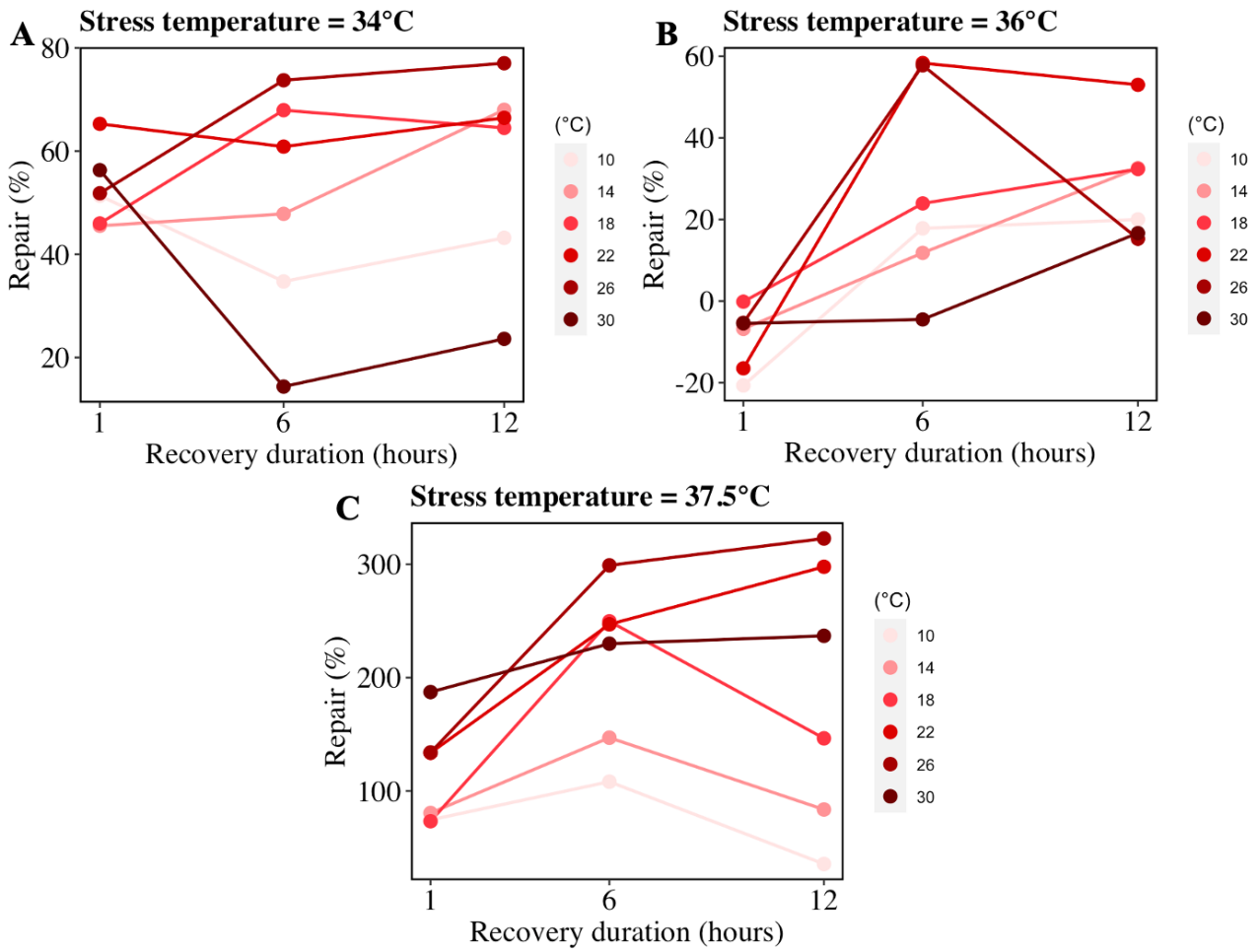

Figure 6.

Relative recovery rates at different temperatures and recovery durations for *Drosophila suzukii* (dataset from Ørsted et al., 2026). Relative recovery (%) is shown as a function of recovery duration (1, 6, and 12 hours) following exposure to three stressful temperatures: 34°C (A), 36°C (B), and 37.5°C (C). Relative recovery rates were calculated in relation to control experiments in which flies were exposed only to the stressful temperatures without intervening recovery periods, allowing baseline injury accumulation to be quantified. Points represent mean values derived from individual thermal failure times (defined as time of heat coma) across experimental replicates. Across all stress temperatures, recovery dynamics generally follow an exponential decay in injury over time. However, the rate and extent of recovery are strongly dependent on the temperature at which recovery occurs. This is reflected in the divergence among curves within each panel, indicating that higher recovery temperatures alter the trajectory of injury reduction. Data are derived from the

dynamic recovery experiments described in Fig. 3C, in which flies were subjected to alternating stressful and permissive thermal regimes.

Discussion

Here, we present a statistical framework for ectothermic organisms that can identify and distinguish temperatures that lead to injury accumulation and ultimately acute failure (stressful) from those that allow recovery and support physiological homeostasis (permissive). We show how to predict these injury-repair dynamics over time under fluctuating temperatures using thermal failure data alone.

While some studies have demonstrated how ectotherms recover from a sublethal amount of thermal stress, i.e. repair (Nedvěd et al., 1998; Colinet et al., 2015; Kovacevic et al., 2019), few have considered this is terms of the predictable 'thermal dose' as in the TDT framework (Jørgensen et al., 2019; Jørgensen et al., 2021; Jørgensen et al., 2022; Faber et al., 2024; Faber et al., 2026a). Only a few studies have experimentally investigated how repair and injury generation vary when ectotherms experience fluctuating temperatures (Ørsted et al., 2022; Buckley et al., 2025; Faber et al., 2026a; Ørsted et al., 2026). Here we demonstrate that under such conditions repair can significantly counter injury accumulation and thus alter predictions of thermal failure (Fig. 4-5). Frameworks that neglect repair may therefore misrepresent predictions of both the rate and extent of thermal injury accumulation when modelled over temporal scales where temperatures fluctuate between stressful and permissive ranges (Arnold et al., 2025). More broadly, most existing thermal stress frameworks either ignore repair or treat injury generation and repair as separate processes, limiting their ability to capture the dynamic balance between injury and recovery under fluctuating temperatures.

In both models introduced here, injury and repair are assumed to operate continuously across all temperatures, and failure occurs when a fixed dose of injury is reached. In this perspective, the

apparent additivity that has been empirically demonstrated for both injury accumulation in fish, plants, and insects (Fry et al., 1946; Jørgensen et al., 2021; Ørsted et al., 2022; Faber et al., 2024; Faber et al., 2026a) and for repair in insects (Ørsted et al., 2026) can be understood as arising from the balance between two opposing antagonistic processes. At stressful temperatures, injury accumulates because injury rates exceed repair rates by many orders of magnitudes, whereas at permissive temperatures repair dominates, resulting in net recovery (Ørsted et al., 2022; Ørsted et al., 2026). Thus, additivity does necessarily not imply the absence of either process but rather reflects conditions where one process dominates the other. Hence, when organisms are exposed to sufficiently broad temperature ranges and exposure durations, the balance of these processes can be statistically inferred from thermal failure data alone (Fig. 1) even though they cannot be directly observed. More generally, both modelling approaches provide a means of estimating injury accumulation and repair dynamics from virtually any thermal exposure history, including complex and naturally fluctuating temperature regimes. This creates opportunities to infer these processes under ecologically realistic thermal conditions, overcoming a major limitation of previous frameworks that require injury and repair parameters to be derived from highly controlled laboratory experiments (Jørgensen et al., 2019; Ørsted et al., 2022; Faber et al., 2024; Ørsted et al., 2026; Arnold et al., 2025).

Our two models resolve these injury and recovery dynamics at different levels of resolution. The non-parametric TDT model is efficient for identifying permissive and stressful thermal ranges across heterogeneous experimental datasets. In the case of *L. gibba*, where exposure histories are relatively simple and do not vary strongly in temporal structure, the model performs well in describing how different temperatures contribute to net injury accumulation. Accordingly, the model output support the results of Faber et al., (2026a), separating temperatures that result in net injury accumulation and those that do not. Hence, the model is useful for integrating diverse exposure histories within a single

statistical framework, relaxing requirements of temperature control during experiments and deriving inference of datasets that differ in duration and/or temperature combinations. However, the model assumes that the temporal order of thermal exposure is irrelevant, but this assumption is most valid for when temperatures are stressful, and injury accumulation dominates (Jørgensen et al., 2021; Ørsted et al., 2026). Accordingly, the model is most reliable when applied to datasets with relatively simple structured temperature sequences, where net effects dominate over dynamic feedback between injury and repair.

Modelling how repair rates depend on initial injury levels

One potential drawback of the non-parametric model, is that it does not account for repair processes being injury dependent, meaning that net repair at a given temperature can vary depending on the prior accumulated injury (Feder & Hofmann, 1999; Kültz, 2005; Jager et al., 2011; Jager & Ashauer, 2018**;** Mangold-Döring et al., 2023; Fig. 6). As a result, the model may misestimate net injury when exposure histories differ in their temporal structure, even if total exposure times are similar. This limitation is apparent in the *D. suzukii* dataset, for example where temperature profiles alternate between stressful and permissive temperatures in repeated cycles (Fig. 3E). This explains why the model estimates significant injury at 10 and 14 °C (Fig. 4B) even though recovery is present and detectable at these temperatures in this dataset (Ørsted et al., 2026).

In contrast, our parametric model accounts for the temporal sequence of temperature exposures and the injury dependence of repair, allowing it to capture these dynamics (Fig. 5), but at the cost of requiring more data for robust parameter estimation. While split-dose and recovery experiments have provided valuable insights of the balance between thermal injury and repair, such experiments are specifically designed to isolate injury and recovery processes. By contrast, the present framework

514 infers these processes directly from survival outcomes under arbitrary thermal histories, where injury
515 accumulation and repair occur simultaneously. In this model, net injury is determined by the balance
516 and interaction between injury accumulation and repair, such that identical temperatures can produce
517 different outcomes depending on the sequence, duration, and intensity of exposure. Accordingly,
518 repair is modelled as a temperature-dependent, injury-dependent process consistent with similar
519 established toxicokinetic–toxicodynamic theory (e.g., GUTS; Jager et al., 2011; Jager & Ashauer,
520 2018; Mangold-Döring et al., 2023), which in its standard formulation assumes temperature-
521 independent kinetics. This extension results in an exponential decay of injury capturing a diminishing
522 rate of repair as the system approaches homeostasis which aligns well with the empirical trends shown
523 here (Fig. 6). In contrast, approaches that assume linear repair implicitly treat recovery as independent
524 of injury state (Ørsted et al., 2022; Arnold et al., 2025; Ørsted et al., 2026), which may provide a
525 useful approximation over limited conditions, similar to the non-parametric TDT model introduced
526 here, but does not capture this injury-state dependence. Importantly, for both models introduced here
527 there is no imposed fixed critical temperature (T_c) at which injury and repair rates are equal. Instead,
528 T_c emerges from the intersection of injury and repair rates, allowing the boundary between permissive
529 and stressful temperatures to be objectively estimated directly from thermal failure or mortality data.
530 For the parametric model that accounts for the injury dependence of repair, this enables reconstruction
531 of full injury trajectories under arbitrary thermal histories and prediction of how rapidly organisms
532 approach thermal failure. Because both processes are inferred jointly within a single likelihood
533 framework, the model accounts for the joint uncertainty between both processes.
534

535 **Assumptions and limitations of parametric injury-repair model**

536 Parameter estimation of the parametric injury-repair model requires extensive data as injury and
537 repair are treated as latent processes and this limits the complexity of the equations that can be

supported. Nonetheless, equation six provides a biologically motivated and statistically robust description of these dynamics and should be applicable for ectothermic organisms in general. However, there is still more nuance and complexity that the framework does not yet account for.

The parametric model assumes that repair acts proportionally to the current level of injury and can thus only reduce existing injury, similar to the GUTS framework (Jager et al., 2011; Jager & Ashauer, 2018; Mangold-Döring et al., 2023). However, it might be the case that repair efficiency declines at high levels of injury, e.g., after irreversible injury. Likewise, the rate of further injury accumulation may decrease as the proportion of functional tissue available to sustain additional damage becomes reduced. These effects are not reflected in the current model, as the dataset used was not designed to resolve such dynamics and therefore does not support more complex formulations. For simplicity, here we force the model to cap injury predictions at the failure threshold ($I = 1$) to reflect this to some extent. Explicitly incorporating injury-dependent limits on the rate of repair at the full injury spectrum thus remains an important step toward improving the biological realism of the framework.

Another potentially influential factor, currently not accounted for, is thermal acclimation and heat hardening which are distinct processes expected to influence injury and repair dynamics in ectotherms (Willot et al., 2022; Ørsted et al., 2022; Arnold et al., 2025; Faber et al., 2026b). Acclimation typically occurs over longer timescales and reflects more permanent shifts in thermal tolerance, whereas heat hardening is a rapid, short-term response induced by brief exposure to high temperatures (Precht et al., 1973; Bowler, 2005; Bilyk et al., 2012). These processes are temperature dependent and differ in both their temporal dynamics and thermal sensitivity. However, datasets that allows these effects to be estimated and incorporated into a unified modelling framework are currently lacking. While the dataset used to fit the parametric model here is relatively complex, it still represents controlled

laboratory conditions (Fig. 3). At least one of the experiments in the dataset yielded apparent recovery beyond 100% injury, suggesting a hardening response (Ørsted et al., 2026). The current framework cannot account for these confounding effects, highlighting the need for studies that explicitly quantify how acclimation and hardening influence injury accumulation and repair. Incorporating these processes will be an important step towards improving predictions of ectotherm mortality under natural thermal regimes.

The functions for describing injury ($f(T)$) and repair ($r(T)$) dynamics used in this study were chosen based on their simplicity to enable robust parameter estimates as well as the previously documented temperature responses for injury (Rezende et al., 2014; Jørgensen et al., 2019; Jørgensen et al., 2021; Ørsted et al., 2022; Cook et al., 2024; Faber et al., 2024; Buckley et al., 2025; Arnold et al., 2025) and repair in ectotherms (Ørsted et al., 2022; Arnold et al., 2025; Ørsted et al., 2026). However, these formulations can easily be modified and can be replaced by alternative temperature-response functions. Because the model operates at the level of individual observations, future versions could readily incorporate alternative error structures (e.g. Bullard et al., 2026), hierarchical variance components, or random effects to account for variation among individuals, populations, or experimental conditions. The same modelling framework could also be applied to predict population levels by linking injury dynamics to survival probabilities or population decline directly (Rezende et al., 2014), while using the same underlying differential equation shown here.

Application and data requirements

Estimating parameters in our model requires datasets that capture both the temperature dependence of injury and repair, as well as their interaction through time. Consequently, experiments should span a broad range of temperatures and exposure durations, including both permissive and stressful

586 conditions. Estimation of the injury function ($f(T)$) requires thermal failure observations across
587 several stressful temperatures, while estimation of the repair function ($r(T)$) requires recovery data
588 spanning a wider range of temperatures because repair is expected to exhibit a unimodal thermal
589 response. Because repair depends on the current level of injury, informative datasets must also
590 generate variation in injury levels. This can be achieved through exposure profiles that alternate
591 between stressful and permissive temperatures while varying the duration of exposures within both
592 thermal ranges. This variation is necessary to estimate how repair depends on both temperature and
593 injury level, and to resolve how injury and repair jointly determine net injury dynamics through time.
594 In practice, model performance will be strongest when fitted to datasets that resemble the temporal
595 structure and thermal variability of the conditions under which predictions are required.
596
597 The framework is highly relevant for assessing the biological consequences of current and future
598 climate change across ectothermic organisms. By coupling the framework with biophysical and
599 microclimate models that predict organism-specific thermal exposures (Kearney & Porter, 2009;
600 Kearney & Porter, 2020), current and future environmental temperature variation can be translated
601 directly into predicted injury accumulation and repair dynamics (Noble et al., 2026). These injury
602 trajectories can be integrated with Dynamic Energy Budget or population models to scale
603 physiological stress to life-history traits, population growth, and species interactions (Kooijman,
604 2010; Nisbet et al., 2000; Bimler et al., 2018; Bowler et al., 2022). In addition, the framework
605 provides quantitative estimates of injury accumulation and repair parameters that can be compared
606 across species, populations, and life stages. Such comparisons may help us understand how thermal
607 tolerance evolves and adapts across ectotherms, and how temporal differences in injury accumulation
608 and repair capacity shape resilience to environmental change and increasingly extreme heat events.
609

Conflict of interest

This work has no conflict of interests.

Author contributions

AHF, PB, BKE, JO and MØ planned and designed the study. PB developed the equations for both models, while AHF wrote the R scripts and performed the data analyses. AHF prepared the first draft of the manuscript under the supervision of MØ, and all authors contributed to manuscript revision and approved the final version.

Data availability

The data used in this manuscript will be made available on https://figshare.com upon acceptance of the manuscript for publication.

Funding

This work was supported by the Independent Research Fund Denmark (grants DFF-1026-00173B to BKE, DFF-4251-00089B to MØ, and DFF-9040-00348B to JO) and the Novo Nordisk Foundation (grant NNF23OC0082599 to MØ).

Supplementary material

Table S1.

Parameter estimates of the parametric thermal injury repair model. The values are given as maximum likelihood estimates ± standard error (SE). During optimisation, parameters were constrained to biologically realistic ranges: β = 0.69 – 1.15 (corresponding to Q_{10} values between 10^3 and 10^5) , α = 30 – 60 °C, r_{ref} = 10^{-6} – 10^{-1} h^{-1}, E = 0.05 – 4.0 eV, Eh = 0.2 – 15.0 eV, Th = 1 – 31 °C.

Parameters	Estimate	Standard error	Unit
β	0.911	0.010	-
α	45.22	0.10	°C
r_{ref}	0.000031	0.000005	$Hour^{-1}$
E	1.398	0.333	eV
Eh	4.199	0.706	eV
Th	24.89	1.38	°C
Standard deviation (σ)	0.24	0.005	-

References

Angilletta Jr, M. J. (2009). Thermal adaptation: a theoretical and empirical synthesis. Oxford Univ. Press.

Arnold, P. A., Noble, D. W., Nicotra, A. B., Kearney, M. R., Rezende, E. L., Andrew, S. C., ... & Bennett, J. M. (2025). A framework for modelling thermal load sensitivity across life. Global Change Biology, 31(7), e70315.

Bilyk, K. T., Evans, C. W., & DeVries, A. L. (2012). Heat hardening in Antarctic notothenioid fishes. Polar biology, 35(9), 1447-1451.

Bimler, M. D., Stouffer, D. B., Lai, H. R., & Mayfield, M. M. (2018). Accurate predictions of coexistence in natural systems require the inclusion of facilitative interactions and environmental dependency. Journal of Ecology, 106(5), 1839-1852.

Bowler, K. (2005). Acclimation, heat shock and hardening. Journal of Thermal Biology, 30(2), 125-130.

Bowler, C. H., Weiss-Lehman, C., Towers, I. R., Mayfield, M. M., & Shoemaker, L. G. (2022). Accounting for demographic uncertainty increases predictions for species coexistence: A case study with annual plants. Ecology Letters, 25(7), 1618-1628.

Briceño, V. F., Arnold, P. A., Cook, A. M., Courtney Jones, S. K., Gallagher, R. V., French, K., ... & Leigh, A. (2025). Drivers of thermal tolerance breadth of plants across contrasting biomes. Journal of Ecology.

Buckley, L.B., Huey, R.B. & Ma, C.-S. (2025). How damage, recovery, and repair alter the fitness impacts of thermal stress. Integr Comp Biol, icaf019.

Bullard, G. W., Buckley, L. B., & Kingsolver, J. G. (2026). Moving beyond mean thermal death times to assess organismal responses to stressful temperatures. bioRxiv, 2026-01.

668

669 Colinet, H., Sinclair, B.J., Vernon, P. & Renault, D. (2015). Insects in fluctuating thermal
670 environments. *Annual Review of Entomology*, 60, 123–140.

671

672 Cook, A. M., Rezende, E. L., Petrou, K., & Leigh, A. (2024). Beyond a single temperature threshold:
673 Applying a cumulative thermal stress framework to plant heat tolerance. Ecology Letters, 27(3),
674 e14416.

675

676 Cossins A. R., Bowler K. (1987). Temperature biology of animals. London: Chapman and Hall.

677

678 Diamond, S. E. (2017). Evolutionary potential of upper thermal tolerance: biogeographic patterns and
679 expectations under climate change. Annals of the New York Academy of Sciences, 1389(1), 5-19.

680

681 Dowd, W.W., King, F.A. & Denny, M.W. (2015). Thermal variation, thermal extremes and the
682 physiological performance of individuals. *Journal of Experimental Biology*, 218, 1956–1967.

683

684 Faber, A. H., Møller, F. D., Ørsted, M., Ehlers, B. K., & Overgaard, J. (2026a). Separating good from
685 bad–a methodological assessment of the critical temperature that separates stressful and permissive
686 temperatures in ectotherms.

687

688 Faber, A. H., Thompson, J. D., Gauthier, P., & Ehlers, B. K. (2026b). The scent of survival in a
689 warming world: how monoterpenes drive thermal adaptation in thyme (preprint). EcoEvoRxiv.
690 https://doi.org/10.32942/X2X67Q

691

692 Faber, A. H., Ørsted, M., & Ehlers, B. K. (2024). Application of the thermal death time model in
693 predicting thermal damage accumulation in plants. Journal of Experimental Botany, 75(11), 3467-
694 3482.
695
696 Feder, M. E., & Hofmann, G. E. (1999). Heat-shock proteins, molecular chaperones, and the stress
697 response: evolutionary and ecological physiology. Annual review of physiology, 61(1), 243-282.
698
699 Fitter, A. H., & Hay, R. K. (2012). Environmental physiology of plants. Academic press.
700
701 Fry, F.E.J., Hart, J.S. & Walker, K.F. (1946). Lethal temperature relations for a sample of young
702 speckled trout, Salvelinus fontinalis. Publications of the Ontario Fisheries Research Laboratory, 9–
703 35.
704
705 Hoffmann, G. E., & Todgham, A. E. (2010). Living in the now: physiological mechanisms to tolerate
706 a rapidly changing environment. Annual review of physiology, 72(1), 127-145.
707
708 Huey, R. B., & Kingsolver, J. G. (1989). Evolution of thermal sensitivity of ectotherm performance.
709 Trends in ecology & evolution, 4(5), 131-135.
710
711 IPCC. (2023) In: Core Writing Team, H. Lee & J. Romero (Eds) Climate change 2023: synthesis
712 report. Contribution of Working Groups I, II and III to the sixth assessment report of the
713 Intergovernmental Panel on Climate Change. Geneva, Switzerland: IPCC, PP. 35-115.
714

715 Jager, T., Albert, C., Preuss, T. G., & Ashauer, R. (2011). General unified threshold model of
716 survival-a toxicokinetic-toxicodynamic framework for ecotoxicology. Environmental science &
717 technology, 45(7), 2529-2540.
718
719 Jager, T., & Ashauer, R. (2018). Modelling survival under chemical stress: A comprehensive guide
720 to the GUTS framework.
721
722 Jørgensen, L.B., Malte, H. & Overgaard, J. (2019). How to assess *Drosophila* heat tolerance:
723 Unifying static and dynamic tolerance assays to predict heat distribution limits. *Functional Ecology*,
724 33, 629–642.
725
726 Jørgensen, L.B., Malte, H., Ørsted, M., Klahn, N.A. & Overgaard, J. (2021). A unifying model to
727 estimate thermal tolerance limits in ectotherms across static, dynamic and fluctuating exposures to
728 thermal stress. Scientific Reports, 11, 12840.
729
730 Jørgensen, L. B., Ørsted, M., Malte, H., Wang, T., & Overgaard, J. (2022). Extreme escalation of
731 heat failure rates in ectotherms with global warming. Nature, 611(7934), 93-98.
732
733 Kearney, M., & Porter, W. (2009). Mechanistic niche modelling: combining physiological and spatial
734 data to predict species' ranges. Ecology letters, 12(4), 334-350.
735
736 Kearney, M. R., & Porter, W. P. (2020). NicheMapR–an R package for biophysical modelling: the
737 ectotherm and dynamic energy budget models. Ecography, 43(1), 85-96.
738

739 Kingsolver, J.G. & Buckley, L.B. (2017). Quantifying thermal extremes and biological variation to
740 predict evolutionary responses to changing climate. *Philosophical Transactions of the Royal Society*
741 *B: Biological Sciences*, 372, 20160147.
742
743 Kooijman, S. A. L. M. (2010). Dynamic energy budget theory for metabolic organisation. Cambridge
744 university press.
745
746 Kovacevic, A., Latombe, G. & Chown, S.L. (2019). Rate dynamics of ectotherm responses to thermal
747 stress. Proceedings of the Royal Society B: Biological Sciences, 286, 20190174.
748
749 Kristensen, K., Nielsen, A., Berg, C. W., Skaug, H., & Bell, B. M. (2016). TMB: automatic
750 differentiation and Laplace approximation. Journal of statistical software, 70, 1-21.
751
752 Kültz, D. (2005). Molecular and evolutionary basis of the cellular stress response. Annu. Rev.
753 Physiol., 67(1), 225-257.
754
755 Lutterschmidt, W. I., & Hutchison, V. H. (1997). The critical thermal maximum: data to support the
756 onset of spasms as the definitive end point. Canadian Journal of Zoology, 75(10), 1553-1560.
757
758 Malusare, S. P., Zilio, G., & Fronhofer, E. A. (2023). Evolution of thermal performance curves: A
759 meta-analysis of selection experiments. Journal of Evolutionary Biology, 36(1), 15-28.
760

761 Mangold-Döring, A., Baas, J., van den Brink, P. J., Focks, A., & van Nes, E. H. (2023).
762 Toxicokinetic–toxicodynamic model to assess thermal stress. Environmental Science & Technology,
763 57(50), 21029-21037.
764
765 Nedvěd, O., Lavy, D. & Verhoef, H.A. (1998). Modelling the time-temperature relationship in cold
766 injury and effect of high-temperature interruptions on survival in a chill-sensitive Collembolan.
767 Functional Ecology, 12, 816–824.
768
769 Nisbet, R. M., Muller, E. B., Lika, K., & Kooijman, S. A. L. M. (2000). From molecules to ecosystems
770 through dynamic energy budget models. Journal of animal ecology, 913-926.
771
772 Noble, D. W., Mayfield, M. M., Hoffmann, A. A., Chen, Z. H., Lade, S. J., Bai, X., ... & Kearney,
773 M. R. (2026). A systems modelling approach to predict biological responses to extreme heat. Trends
774 in ecology & evolution.
775
776 Precht, H., Christophersen, J., Hensel, H. and Larcher, W. (1973). In Temperature and Life, pp. 302-
777 348. Springer.
778
779 Rezende, E.L., Castañeda, L.E. & Santos, M. (2014). Tolerance landscapes in thermal ecology.
780 Functional Ecology, 28, 799–809.
781
782 Schulte, P. M., Healy, T. M., & Fangue, N. A. (2011). Thermal performance curves, phenotypic
783 plasticity, and the time scales of temperature exposure. Integrative and comparative biology, 51(5),
784 691-702.

Stocker, C.W., Bamford, S.M., Jahn, M., Mazué, G.P.F., Pettersen, A.K., Ritchie, D., *et al.* (2024). The Effect of Temperature Variability on Biological Responses of Ectothermic Animals—A Meta-Analysis. *Ecology Letters*, 27, e14511.

Sunday, J. M., Bates, A. E., & Dulvy, N. K. (2011). Global analysis of thermal tolerance and latitude in ectotherms. Proceedings of the Royal Society B: Biological Sciences, 278(1713), 1823-1830.

Vasseur, D.A., DeLong, J.P., Gilbert, B., Greig, H.S., Harley, C.D.G., McCann, K.S., *et al.* (2014). Increased temperature variation poses a greater risk to species than climate warming. *Proceedings of the Royal Society B: Biological Sciences*, 281, 20132612.

Willot, Q., Ørsted, M., Damsgaard, C., & Overgaard, J. (2022). Thermal-death-time model as a tool to analyze heat tolerance, acclimation, and biogeography in ants. Myrmecological News, 32.

Ørsted, M., Jørgensen, L. B., Hůla, P., & Overgaard, J. (2026). Integrating Physiological Rates of Thermal Stress and Repair Predicts Heat Failure During Temperature Fluctuations. Ecology Letters, 29(5), e70398.

Ørsted, M., Jørgensen, L.B. & Overgaard, J. (2022). Finding the right thermal limit: a framework to reconcile ecological, physiological and methodological aspects of CTmax in ectotherms. Journal of Experimental Biology, 225, jeb244514.